Experimental Realization of Stokes Modes of the Pipe by Lorentz Excitation *

A. Pysik and J. Heber

Institut für Festkörperphysik der Technischen Hochschule Darmstadt

Z. Naturforsch. **47a**, 1097–1104 (1992); received August 7, 1992

The complete set of the Stokes modes of the pipe was first given by Brosa and Boberg. Two of these modes for an incompressible fluid were now realized in a transparent tube and detected by a laser light cut. Their velocity fields and lifetimes were compared with the theoretical predictions, and good agreement was found. The modes were generated by Lorentz force fields of appropriate symmetry induced by an electrical current through the fluid and external magnetic fields. For higher excitation intensities effects of mode coupling could be observed.

I. Introduction

The onset of turbulence in a pipe is still an open problem. Experimentally it is known that the laminar flow through a pipe undergoes a transition to turbulence if it becomes too fast, usually at Reynolds numbers around 2000. It is further known that the critical Reynolds numbers can reach much larger values depending on the degree of perfection of the experiment, e.g., if very straight and smooth pipes are used, if the inlet of the pipe is favorably shaped, and if the system is well isolated from mechanical vibrations [1, 2]. These experimental findings have a theoretical counterpart in the fact that the laminar Hagen-Poisseuille flow remains stable under a linear instability analysis at any flow velocity [3]. Only a nonlinear instability analysis shows an amplification of certain perturbations [4]. But it is not simple to correlate these theoretical results with the experimental findings [5].

For concrete problems, such as the flow of an incompressible liquid in a pipe, it is often very useful to approximate the hydrodynamic equations by a finite system of ordinary differential equations using Galerkins method. In this method the velocity field $\boldsymbol{u}(\boldsymbol{r}, t)$ is represented as a series expansion

$$\boldsymbol{u}(\boldsymbol{r}, t) = \sum_{\mu} c_{\mu}(t)\, \boldsymbol{s}_{\mu}(\boldsymbol{r}), \tag{1}$$

where $c_{\mu}(t)$ are timedependent coefficients and $s_{\mu}(\boldsymbol{r})$ are the eigenfunctions of the linearized problem. Linearization for $\boldsymbol{u}(\boldsymbol{r}, t) \to 0$ gives the so-called Stokes modes of a given boundary value problem. The complete set of Stokes modes for the pipe was first given by Brosa [6], and Boberg and Brosa [7]. By the Galerkin method and using the Stokes modes, Boberg and Brosa [7] gave a new and quite interesting theoretical interpretation of the onset of turbulence in a pipe by mode coupling due to the nonlinear term $(\boldsymbol{u}\nabla)\boldsymbol{u}$ in the Navier-Stokes equation.

The aim of this paper is to realize some of the Stokes modes of the pipe experimentally and to study their properties. In Chapt. II we give a short mathematical derivation of the Stokes modes. Chapter III describes the experimental set-up, and the method of their generation. The discussion of the experimental results is given in the final Chapter. IV.

II. The Stokes Modes

The derivation of the Stokes modes for an incompressible fluid can start from the appropriate Navier-Stokes equation

$$\varrho \cdot \partial \boldsymbol{u}'/\partial t' + \varrho(\boldsymbol{u}', \nabla')\boldsymbol{u}' = -\nabla' p' - \eta \nabla' \times \nabla' \times \boldsymbol{u}'. \tag{2}$$

The notations are $\boldsymbol{u}'(\boldsymbol{r}', t')$ = velocity field, ϱ = density, η = viscosity, $p'(\boldsymbol{r}')$ = pressure.

To make the problem independent of the radius R of the pipe and of the special physical properties of the fluid, it is convenient to introduce a dimensionless Navier-Stokes equation by means of the transforma-

* This work was supported by Röhm GmbH Chemical Company, Darmstadt, and Vacuumschmelze GmbH, Hanau, FRG.

Reprint requests to Prof. Dr. J. Heber, Institut für Festkörperphysik der Technischen Hochschule, W-6100 Darmstadt, FRG.

0932-0784 / 92 / 1100-1097 $ 01.30/0. – Please order a reprint rather than making your own copy.

tions:

$$\boldsymbol{r} = \boldsymbol{r}'/R;\ t = t'\,v/R^2;\ p = p'/(\varrho\, v^2/R^2);\ u = u'\,R/v; \quad (3)$$

$v = \eta/\varrho$ denotes the kinematic viscosity.

This way all distances are measured in units of the radius R of the pipe, the time in units of R^2/v, and the pressure in units of $\varrho\, v^2/R^2$. In contrast to [7] we do not relate the velocities and pressures to a more or less arbitrary velocity $U_0(r=0)$ of an additional Hagen-Poiseuille flow. So the Reynolds number of this flow does not show up any more, and U_0 can be set to zero without mathematical complications, (2) in [7].

The Navier-Stokes equation for the incompressible fluid transforms then into

$$\partial \boldsymbol{u}/\partial t + (\boldsymbol{u}\,\boldsymbol{\nabla})\,\boldsymbol{u} = -\boldsymbol{\nabla} p - \boldsymbol{\nabla} \times \boldsymbol{\nabla} \times \boldsymbol{u}. \quad (4)$$

Linearization for $u \to 0$ means that the term $(\boldsymbol{u}\,\boldsymbol{\nabla})\,\boldsymbol{u} \sim \boldsymbol{u}^2$ can be neglected, and we end up with the Stokes equation

$$\partial \boldsymbol{u}/\partial t = -\boldsymbol{\nabla} p - \boldsymbol{\nabla} \times \boldsymbol{\nabla} \times \boldsymbol{u}. \quad (5)$$

The solutions of this equation can be split up into a time- and a space-dependent factor:

$$\boldsymbol{u}_\mu(\boldsymbol{r}, t) = a_\mu(t) \cdot \boldsymbol{s}_\mu(\boldsymbol{r}). \quad (6)$$

The index μ labels the different modes – the so-called Stokes modes – of a given boundary value problem. Generally, $a_\mu(t)$ can be an exponential with complex argument [6]. In the case of an infinitely long pipe filled with an incompressible fluid with no free surfaces, the argument has to be real, because there are no storage capacities for potential energy necessary for oscillations. So the Stokes modes become pure relaxation modes with a time dependence of the form

$$a_\mu(t) = \exp[-\alpha_\mu^2\, t]. \quad (7)$$

The boundary conditions for the Stokes functions $\boldsymbol{s}_\mu(\boldsymbol{r}) = \boldsymbol{s}_\mu(r, \varphi, z)$ of the pipe are:

1. The velocity $\boldsymbol{u}(r, t)$ has to be zero at the wall of the pipe:

$$\boldsymbol{s}_\mu(r = 1, \varphi, z) = 0. \quad (8)$$

2. The velocity field has to be unique in the azimuth angle φ:

$$\boldsymbol{s}_\mu(r, \varphi, z) = \boldsymbol{s}_\mu(r, \varphi + 2\pi, z). \quad (9)$$

3. The velocity field can be periodic along the axis of the tube with a period $0 < L < \infty$:

$$\boldsymbol{s}_\mu(r, \varphi, z) = \boldsymbol{s}_\mu(r, \varphi, z + L). \quad (10)$$

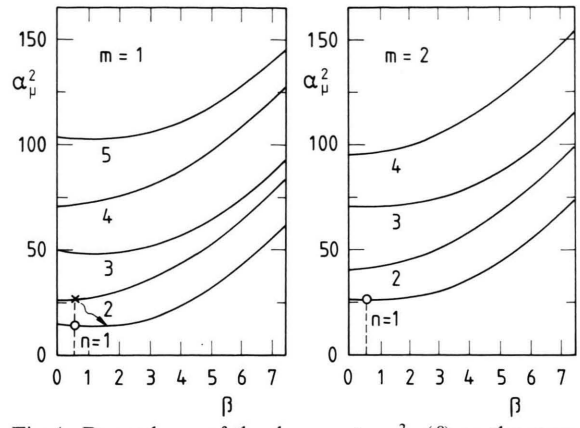

Fig. 1. Dependence of the decay rates $\alpha_{m,n}^2(\beta)$ on the wave-vector $\beta = 2\pi l/L$. Parameters are the azimuthal and radial node indices m, and n, respectively. o: realized modes, ×: tried, but not succeeded.

The complete set of Stokes functions [6, 7] has the form

$$\boldsymbol{s}_\mu(\boldsymbol{r}) = [-i\,u(r)\,\boldsymbol{e}_r + v(r)\,\boldsymbol{e}_\varphi + w(r)\,\boldsymbol{e}_z] \cdot \exp(\mathrm{i}m\varphi + i\beta z) \quad (11)$$

with the components

$$\begin{aligned} u(r) &= A\,J_m(\gamma r)\,m/r + B\,\gamma\,J_m'(\gamma r) &&+ C\,\beta\,I_m'(\beta r), \\ v(r) &= A\,\gamma\,J_m'(\gamma r) &&+ B\,J_m(\gamma r)\,m\,\beta/r + C\,I_m(\beta r)\,m/r, \\ w(r) &= &&- B\,J_m(\gamma r)\,\gamma^2 + C\,\beta\,I_m(\beta r), \end{aligned} \quad (12)$$

and the abbreviations

$$\gamma^2 = \gamma_\mu^2 = \alpha_\mu^2 - \beta^2, \quad \beta = 2\pi l/L, \quad l = 0, 1, 2, \ldots. \quad (13)$$

The azimuthal and axial dependencies are purely periodic. The radial part is given by linear combinations of the standard and modified Bessel functions J_m and I_m, respectively. The index μ is a tripel index

$$\mu = m, n, \beta. \quad (14)$$

$m = 0, \pm 1, \pm 2, \ldots$ azimuthal node index,
$n = 1, 2, 3, \ldots$ radial node index,
$0 \leqq \beta < \infty$ axial wave vector.

The radial node index n labels the solutions of the secular equation for $\alpha_\mu^2 = \alpha_{m,n}^2(\beta)$, which results from the boundary condition (8) for $r = 1$:

$$\begin{aligned} &\beta^2\,\gamma^2\,J_m'^2(\gamma)\,I_m(\beta) + \gamma^3\,\beta\,J_m(\gamma)\,I_m'(\beta)\,J_m'(\gamma) \\ &\qquad - m^2\,\alpha_{m,n}^2(\beta)\,J_m^2(\gamma)\,I_m(\beta) = 0. \end{aligned} \quad (15)$$

The decay rates $\alpha_{m,n}^2(\beta)$ depend on the discrete indices m and n, and they are continuous functions of the

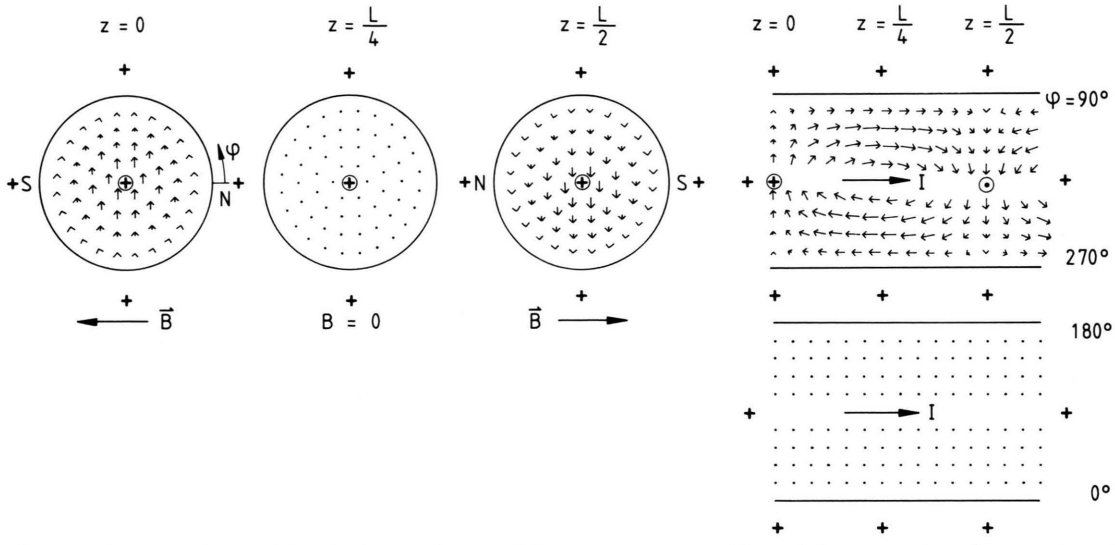

Fig. 2. Excitation scheme of the Stokes mode $m = \pm 1$, $n = 1$; a superposition of the $m = +1$ and $m = -1$ modes with opposite helicities. *I*: electrical current, *B*: magnetic field, *L*: period, $l = 1$.

wavevector $\beta = 2\pi l/L$. These functions have to be calculated numerically. Some of them for $m = 1$ and $m = 2$ are given in Fig. 1 for a number of indices n.

The same condition (8) correlates the constants A, B, and C in (12) such that two of them can be expressed by the third one, which can be interpreted as the arbitrary amplitude of excitation of a given mode. For our calculations of the Stokes functions we took $B = 1$.

The idea behind the Stokes functions is that any velocity field $\boldsymbol{u}(\boldsymbol{r}, t)$ can be expressed by them as a series of symmetry-adapted functions, because they form a complete orthogonal set. In our case of the pipe these functions show in addition a relatively simple analytical form.

III. Experimental

The basic idea to excite the Stokes modes was to use Lorentz-force fields $\boldsymbol{F}(\boldsymbol{r})$ of appropriate symmetry and configuration generated by an electrical current density $\boldsymbol{j}(\boldsymbol{r})$ and an externally applied magnetic field $\boldsymbol{B}(\boldsymbol{r})$.

$$\boldsymbol{F}(\boldsymbol{r}) = \boldsymbol{j}(\boldsymbol{r}) \times \boldsymbol{B}(\boldsymbol{r}). \tag{16}$$

The Lorentz forces act primarily on the charge carriers of the current, but by the impact processes of the charge carriers with the other molecules of the fluid the forces are transferred finally as bulk forces to the fluid.

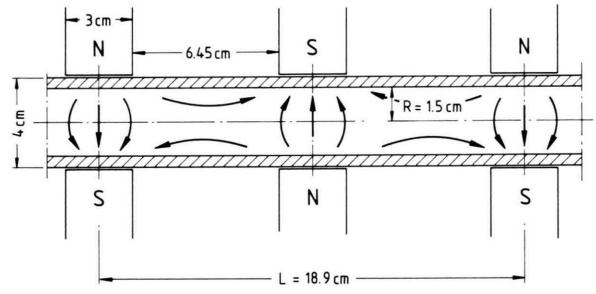

Fig. 3. Realization of a period. $\beta = 0.5$, $L = 4\pi$ in units of R. The arrows indicate the directions of the magnetic fields.

The simplest modes to excite are the modes with $n = 1$, and $m = \pm 1, \pm 2$. The $n = 1$ modes can be excited by a homogeneous current density along the pipe axis. For the $m = \pm 1$ or $m = \pm 2$ modes magnetic dipole or quadrupole fields, respectively are needed perpendicular to the direction of the current. An excitation scheme for the $m = \pm 1$, $n = 1$ mode is shown in Figure 2. The superposition of the $m = +1$ and $m = -1$ modes of opposite helicities results in a plane velocity field. This plane velocity field is very convenient for the excitation as well as for the detection of the modes. For excitation it needs fewer magnets, and for detection a simple laser light cut along the axis permits a full analysis of the velocity field. For the period L a compromise has to be found between an acceptable overall length of the set-up and the

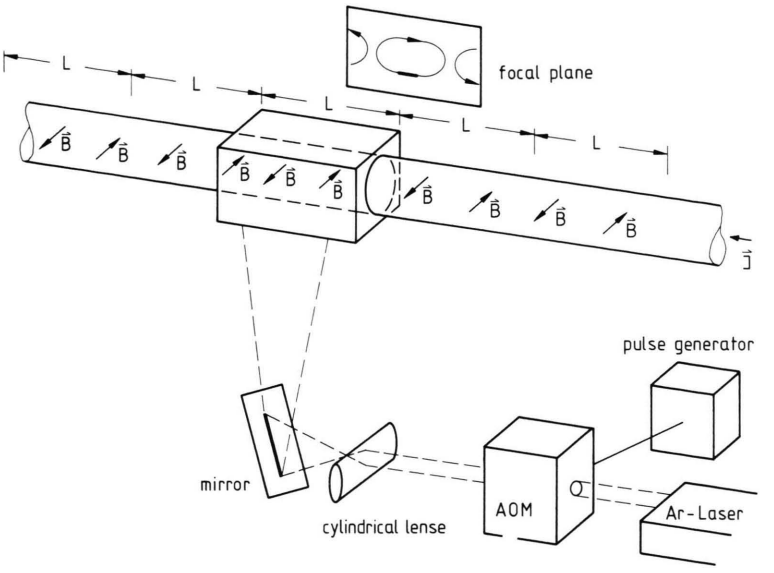

Fig. 4. Scheme of the experimental set-up. I = electric current, B = magnetic field for $m = \pm 1$.

magnetic short-circuit between the neighbouring magnets with alternating polarity. Our realization is shown in Figure 3.

For the $n = 2$ modes we have a node in the radial distribution of the velocity field, i.e. we have to have a corresponding node of the Lorentz-force field, too. This can be realized by a node in the magnetic field distribution, or in the electric current density. The first requirement cannot be realized by externally applied magnetic fields. So we are left with the electric current. An appropriate current distribution can be generated in principle by additional currents along the walls of the pipe in the opposite direction to the main current. These currents were generated by small palladium * coated electrodes inserted into the walls. Although the positions of these electrodes and the desired current distribution were checked up in an electrolytical trough, we were not able to generate the desired $n = 2$ mode. We got only $n = 1$ modes with different β values. The reason is obviously the high damping of the $n = 2$ modes as compared with the $n = 1$ ones (Figure 1). Maybe, with better matched magnetic fields one can succeed.

The scheme of the experimental set-up is given in Figure 4. The pipe system is made of plexiglas (Röhm GmbH, Darmstadt). It consists of three areas with different functions.

1. Detection area: It is made of a block of plexiglas with a cross section of 4×4 cm^2. The borehole in the center is carefully matched to the inner diameter of the adjacent tubes and is polished to optical quality. The plane outer surfaces are necessary to keep the optical distortions of the photographic registration of the velocity field at an acceptable level.
2. Excitation areas: They are located on both sides of the detection area and have the function to generate good quality modes in it. The experiment showed that the propagation property of the given relaxation modes is quite poor. Propagation did not take place in our case over distances longer than about one period L. This had two consequences: The excitation areas could be shortened, but the modes had to be excited within the detection area, too.
3. Relaxation areas: These two areas extend the shown set-up to both sides. Their function is to allow the modes to decay without back reaction on the detection area. Primarily they were designed to have a length of $3L$ each, but because of the bad propagation property of the modes they can be shortened, too.

The pipe was filled with aqueous sulfuric acid (35%, $\sigma = 0.76\ \Omega^{-1}\ \text{cm}^{-1}$) as electrolyte because of the high

* The Pd coating prevents the generation of bubbles due to the electrolysis of water, if alternating directions of the current are used. In one direction the generated H_2 is dissolved in the Pd, and in the other one the generated O_2 recombines with the dissolved H_2.

mobility of the H^+ ions and its low vapor pressure. H^+ ions are the ions with the highest mobility ensuring a high electrical conductivity and low energy dissipation. No thermal convection effects could be observed.

The magnets were made of iron bars of 3×3 cm^2 cross section. The magnetic flux was generated by the permanent-magnetic material NdFeB (Vacodym 351 HR, Vacuumschmelze, Hanau). 4 slabs of $3 \times 3 \times 1$ cm^2 per magnet generated a magnetic field $B \simeq 0{,}1$ T over a distance of 4 cm.

The light cut for the visualization of the velocity field of the modes was generated by an argon laser beam (4 W) expanded by a cylindrical lense. As tracer particles club moss spores (lycopodium bispeduratum) were used. They are light enough to follow the velocity field without distortions, and their light scattering ability is strong enough for photographic registration by a camera with a macroobjective. The exposure time was controlled by chopping the laser beam by an acoustooptic modulator. For a given exposure time the lengths and directions of the traces of the particles on the photographs are a measure of the velocity field. They were digitized by means of a digitizing table and stored in a computer for further data processing. The experimental values of the velocities $\boldsymbol{u}(\boldsymbol{r})$ were compared with the theoretical ones of the Stokes mode $\boldsymbol{s}(\boldsymbol{r})$ calculated for the same positions, and the two velocity fields were fitted one to another by a common amplitude factor a by the least squares method.

$$\boldsymbol{u}(\boldsymbol{r}) = a\,\boldsymbol{s}(\boldsymbol{r}). \tag{17}$$

To demonstrate graphically the quality of the fit the difference velocity field

$$\Delta\boldsymbol{u}(\boldsymbol{r}) = \boldsymbol{u}(\boldsymbol{r}) - a\,\boldsymbol{s}(\boldsymbol{r}) \tag{18}$$

was calculated and plotted, too. To have a quantitative measure of the quality of the fits the mean square deviation σ_a for the amplitude a was calculated, and a χ^2 test [8] has been done, too. By its definition, $\chi^2 \simeq 1$ means pure statistical deviation between theory and experiment, and higher values indicate systematic errors.

To determine the relaxation rates $\alpha^2_{m,n}(\beta)$, a number of velocity fields were fitted at different times t' after excitation, and the resulting amplitudes $a(t')$ were fitted to an exponential decay

$$a(t') = a_0 \exp[-t'/\tau]. \tag{19}$$

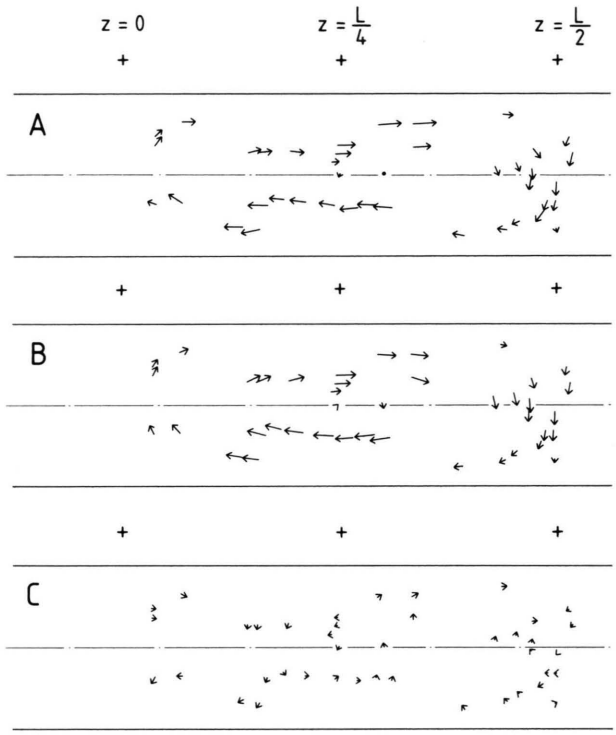

Fig. 5. Analysis of the mode $m = \pm 1$, $n = 1$, $\beta = 0.5$. – A: Digitized particle traces, $\boldsymbol{u}(\boldsymbol{r})$. – B: Stokes field with fitted amplitude, $a\,\boldsymbol{s}(\boldsymbol{r})$. – C: Difference field $\Delta\boldsymbol{u}(\boldsymbol{r}) = \boldsymbol{u}(\boldsymbol{r}) - a\,\boldsymbol{s}(\boldsymbol{r})$. – Current density $j = 40$ mA/cm^2, magnetic field $B = 0.09$ T, excitation time 4 sec, exposure time 0.25 sec, velocity scale: length of the radius R is equivalent to 6 cm/sec.

The experimental decay time τ is related to the dimensionless relaxation rate α^2 by

$$\tau = R^2/\nu\,\alpha^2. \tag{20}$$

IV. Results and Discussion

The numerical data and results of the two modes generated and analyzed are summarized in Table 1.

The analysis of the mode $m = \pm 1$, $n = 1$, $\beta = 0.5$ is shown in Figure 5. Part A shows the experimental velocity field as as measured in the light cut, and part B gives the amplitude-fitted Stokes field for comparison. The difference field in part C shows that the differences between the experimental and theoretical velocities are almost statistical: The arrowheads essentially dominate the picture. Nevertheless, the χ^2-test gives a value of 1.42, indicating some systematic deviations which may be explained by the distortions of the optical imaging at the plexiglas-air interface.

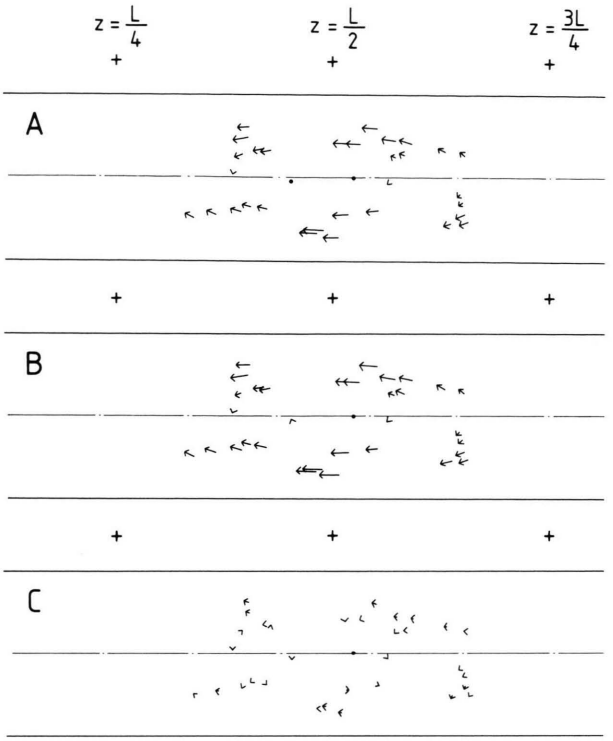

Fig. 6. Analysis of the mode $m = \pm 2$, $n = 1$, $\beta = 0.5$. – A: Digitized particle traces, $\boldsymbol{u}(\boldsymbol{r})$. – B: Stokes field with fitted amplitude, $a\,\boldsymbol{s}(\boldsymbol{r})$. – C: Difference field $\Delta\boldsymbol{u}(\boldsymbol{r}) = \boldsymbol{u}(\boldsymbol{r}) - a\,\boldsymbol{s}(\boldsymbol{r})$. – Current density $j = 60\ \mathrm{mA/cm^2}$, magnetic field $B_{\max} = 0.12$ T, excitation time 3 sec, exposure time 0.25 sec, velocity scale: $R = 6$ cm/sec.

Table 1. Summary of the results for the two modes generated and analyzed. The notations are the same as in the text.

m	n	β	L	τ_{theor} [sec]	α	σ_α	χ^2	τ_{exp} [sec]
±1	1	0.5	4π	9.11	$2.7 \cdot 10^{-3}$	$3.2 \cdot 10^{-4}$	1.42	8.4 ± 0.9
±2	1	0.5	4π	4.98	$5.7 \cdot 10^{-2}$	$2.1 \cdot 10^{-3}$	1.09	5.6 ± 1.6

The similar analysis of the mode $m = \pm 2$, $n = 1$, $\beta = 0.5$ is given in Figure 6. This mode has a twofold azimuthal symmetry. Therefore the velocity fields in the upper and in the lower half of the light cut have the same direction. The difference field again shows more or less statistical deviations between experiment and theory. The statistical character of these errors is demonstrated by the low χ^2-value of only 1.09. The systematic error due to the distortion of the optical imaging at the plexiglas-air interface is expected to be smaller for this mode because of a better scale of optical imaging. Finally, the decay times of both modes

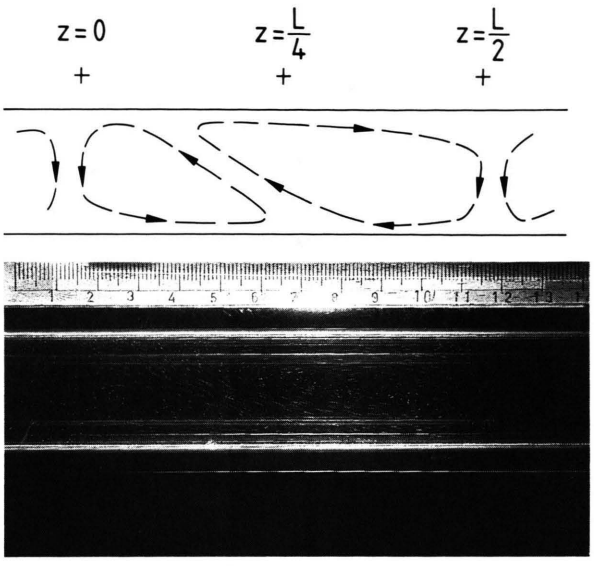

Fig. 7. Deformation of the $m = \pm 1$, $n = 1$, $\beta = 0.5$ mode at higher excitation amplitudes. – A: Photograph – B: sketch of the velocity field. – Current density $j = 890\ \mathrm{mA/cm^2}$, magnetic field $B = 0.09$ T, excitation time 8 sec, exposure time 0.125 sec, time after starting the excitation 10 sec, velocity scale: $R = 12$ cm/sec.

were measured as described in Chapter III. The results given in Table 1 are in good agreement with the theoretical values.

Going to higher excitation amplitudes the modes do not decay uniformly anymore. An example is shown in Fig. 7 for the $m = \pm 1$, $n = 1$, $\beta = 0.5$ mode. For the first seconds of excitation the mode grows and stays stable, but then it starts to decompose under continuing excitation, first into the velocity field shown, and then into more complex unstable and finally also threedimensional flow patterns. The first step of decomposition of the mode into the asymmetric velocity field in Fig. 7 is very reproducible, although the reason for its asymmetry is unclear to us yet:

i) Thermal effects can be ruled out, because the electric heat dissipation in the liquid is uniform, and during the time of the experiment of about $10 \cdots 15$ seconds no heat conduction through the plexiglass walls of the tube (5 mm) can be expected. This is confirmed by the fact that no convection flow could be observed after the experiments.

ii) Moving the magnets up and down by several millimeters did not change the pattern in any way.

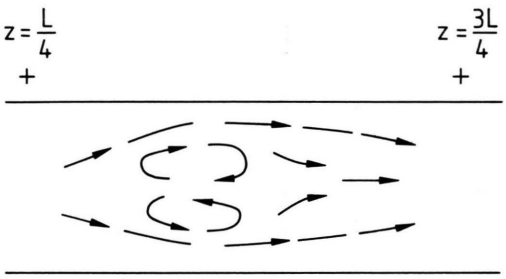

Fig. 8. Sketch of the first step of decomposition of the mode $m = \pm 2$, $n = 1$, $\beta = 0.5$.

iii) Geometrical asymmetries of the pipe in the detection area are expected to be very small because the borehole has been machined on a lathe very carefully. If not small asymmetries of the pipes in the excitation areas are transfered into the detection area, geometrical asymmetry is very unlikely the reason for it, too.

So the reason for the asymmetric velocity field in Fig. 7 looks more like a mode-coupling problem.

The following steps of the decomposition of the mode become more and more irreproducible or chaotic. It looks like a stepwise decay into smaller and smaller structures resembling Kolmogorovs [9] picture of developing turbulence.

The mode $m = \pm 2$, $n = 1$, $\beta = 0.5$ showed a similar decomposition at higher excitation amplitudes. But in this case the first reproducible flow pattern of the decay sketched in Fig. 8 did not show any asymmetry. The following steps of the decomposition into smaller and smaller flow patterns showed the same behaviour as described before.

The dependence of these mode decomposition processes on the excitation intensity is an indication that they result from mode coupling due to the nonlinear term $(\boldsymbol{u}\nabla)\boldsymbol{u} \sim \boldsymbol{u}^2$ in the Navier-Stokes equation, which has been omitted in deriving the Stokes modes. Note that this coupling shows up markedly already at relatively low amplitudes of the modes ($\mathrm{Re} \sim \langle u^2 \rangle^{1/2} R/\nu \approx 5$).

The Galerkin-equations of the dynamics of the Stokes modes have the form [7]

$$\partial c_\mu(t)/\partial t = \sum_{\varkappa,\lambda} W_\mu^{\varkappa\lambda} c_\varkappa(t) \cdot c_\lambda(t) - \alpha_\mu^2 c_\mu(t). \quad (21)$$

The $c_\nu(t)$ are the time-dependent amplitudes of the corresponding Stokes modes $\boldsymbol{s}_\nu(\boldsymbol{r})$, and the $W_\mu^{\varkappa\lambda}$ are the nonlinear mode coupling coefficients given in [7]. The first term at the right hand side describes the nonlinear mode transformations, and the second one the intrinsic decay due to the viscosity of the fluid. The selection rules for the mode coupling coefficients are [7]

$$W_\mu^{\varkappa\lambda} \neq 0 \text{ only for } m_\mu = m_\varkappa + m_\lambda,\ \beta_\mu = \beta_\varkappa + \beta_\lambda. \quad (22)$$

The same selection rules hold for the coupling to the Hagen-Poisseuille flow with $m_{\mathrm{HP}} = \beta_{\mathrm{HP}} = 0$ [7].

In our experiment the period L is well defined by the distances of the magnets along the pipe. So, the dominant starting modes $\varkappa$ and λ generated in our experiment have a well defined wave vector $\beta_\varkappa = \beta_\lambda = 0.5$. According to the selection rules (22) the mode μ generated by the coupling of these modes is expected to have a wave vector $\beta_\mu = \beta_\varkappa + \beta_\lambda = 1$. The decomposing modes in Fig. 7 and Fig. 8 show indeed evidence for an upcoming period reduction by a factor of two as expected from the selection rules for β. For the selection rules of the multipolarity m no clear evidences could be found with our relatively simple experimental set-up. More sophisticated magnetic fields and detection methods would be necessary for this purpose, and to study the mode coupling and mode dynamics generally.

From a thermodynamic point of view, the relaxation of the excited modes can be interpreted as a thermalization process. The Stokes modes are orthogonal collective degrees of freedom of the fluid in the pipe. After Boltzmanns equipartition theorem the kinetic energy per mode at the temperature T amounts to $k_B T/2$.

The externally excited modes are of course "hot modes". According to (21) the hot modes have two channels to decay to their thermal equilibrium energy, which from a macroscopic point of view is almost zero.

i) Intrinsic decay due to the internal friction or viscosity of the fluid. It is proportional to the amplitude of the mode itself and results in a uniform exponential decay of the mode with a decay rate α_μ^2.
ii) decay due to nonlinear mode conversion. In the picture of (21) this means a decay of the modes $\varkappa$ and/or λ due to nonlinear transfer of energy to the mode μ. Because this decay is nonlinear in the mode amplitudes, it is generally nonexponential, and it exhibits a kind of threshold character in the amplitudes under which this channel is ineffective. Due to the different time-dependences of the mode

amplitudes the resulting flow pattern shows a turbulent character.

In the case of our experiment we have $m_\varkappa$, m_λ, $\beta_\varkappa$, and β_λ different from zero. According to the selection rules (22) they can generate a progression of modes with increasing indices (m, n, β), whereby for n no selection rules exist. The mode coupling coefficients $W_\mu^{\varkappa\lambda}$, (14) in [7], are expected to grow generally with increasing indices of the modes because of their increasing vorticities. So the threshold for the nonlinear decay is determined basically by the amplitudes and coupling coefficients of the starting modes. Once this threshold is exceeded, a growing number of higher indexed modes with stronger couplings are generated leading to increasingly smaller and more complex flow patterns, as observed in our experiments. Because of the increasing number of modes involved with generally increasing intrinsic decay rates α_μ^2, this is a transient process of no return, as expected for a thermalization process.

The situation looks somewhat different for a pure Hagen-Poisseuille flow in a pipe. Nonlinear decay can start only with $\beta_\varkappa = \beta_\lambda = 0$, $m_\varkappa = m_\lambda = 0$. According to the selection rules (22) we can expect from this nonlinear selfinteraction only the generation of modes of the kind $(0, n, 0)$, which cannot give rise to turbulence but only to axisymmetric deformations of the parabolic Hagen-Poisseuille velocity profile. So, by the selection rules of mode coupling, i.e. by symmetry, the laminar flow in a pipe is stable at any velocity. But at higher flow velocities, i.e. amplitudes or Reynolds numbers, it becomes metastable against nonsymmetric perturbations, i.e. against "triggering modes" with finite m and β values and of sufficient amplitudes, as discussed in [7] by computer simulations. These triggering modes can be due to external perturbations, deformations of the pipe, etc., down to thermally excited modes. So, in the picture of the Stokes modes the observed rather big difference between the critical Reynolds numbers of the Hagen-Poisseuille flow (~ 2000) and of the investigated Stokes modes (~ 5) can be understood by the discussed symmetry selection rules of mode coupling.

V. Summary and Outlook

It has been shown that the Stokes modes of the pipe derived by Brosa [6], and Boberg and Brosa [7] can be successfully generated by Lorentz force fields. The shape of the modes as well as their decay times are in good agreement with the theoretical calculations. At higher excitation amplitudes the modes show a decomposition into higher modes obviously by nonlinear mode coupling. This effect shows up already at moderate amplitudes of the modes easily obtainable by the proposed method. So the mode coupling responsible for the onset of turbulence can be studied by this method quite conveniently in a flowless tube without having the problem that the Hagen-Poisseuille flow flushes the developing turbulence out of the detection area or even out of the pipe. On the other hand the important problem of the coupling of the modes to the Hagen-Poisseuille flow can obviously not be studied in the flowless tube. In this case perturbations of definite symmetry and duration have to be superimposed on the Hagen-Poisseuille flow. This can be done by electromagnetic Lorentz forces very successfully, too [10, 11].

To study the interesting problem of mode coupling in the flowless pipe in more detail by Lorentz excitation, first of all magnetic fields better matched to the shape of the modes are necessary.

[1] H. Schlichting, Grenzschichttheorie, Verlag G. Braun, Karlsruhe 1982.
[2] T. Sarpkaya, J. Basic Engineering (Trans. ASME, Ser. D) **88,** 589 (1966).
[3] P. Drazin and W. Reid, Hydrodynamic Stability, University Press, Cambridge 1981.
[4] W. Ebeling and Y. L. Klimontovich, Selforganization and Turbulence in Liquids, Teubner Verlagsgesellschaft, Leipzig 1984.
[5] P. K. Sen, D. Venkateswarlu, and S. Maji, J. Fluid Mech. **158,** 289 (1985) and references therein.
[6] U. Brosa, Z. Naturforsch. **41 a,** 1141 (1986).
[7] L. Boberg and U. Brosa, Z. Naturforsch. **43 a,** 697 (1988).
[8] P. R. Bevington, Data Reduction and Error Analysis for the Physical Sciences, McGraw Hill, New York 1969.
[9] A. S. Monin, A. M. Yaglom, Statistical Fluid Mechanics: Mechanis of Turbulence, Vol. I, MIT Press, Cambridge, Massachusetts, 5th Edition 1987.
[10] U. Brosa, Z. Naturforsch. **46 a,** 473 (1991).
[11] E. O. Schulz-Dubois et al., to be published.